Plant Physiology, 2026, 201, 1–15
https://doi.org/10.1093/plphys/kiag191
Published: 28 May 2026
Research article

Plant Physiology®

Drought-responsive TaMIP1 controls root density to confer the tradeoff between grain yield and drought resistance in wheat

Zipei Fan[1,2‡], Xiaosha Tang[1,2‡], Jingyi Wang[1‡], Yang Zhao[1], Wenjing An[1], Yujing Jia[1], Zhixiong Pan[1], Yao Wang[1], Long Li[1], Xinguo Mao[1], Daizhen Sun[2], Jiemeng Xu[3], Matthew Paul Reynolds[3], Ruilian Jing[1]*, and Chaonan Li[1]*

[1]State Key Laboratory of Crop Gene Resources and Breeding, National Key Facility for Crop Gene Resources and Genetic Improvement, Institute of Crop Sciences, Chinese Academy of Agricultural Sciences, Beijing 100081, China

[2]College of Agriculture, Shanxi Agricultural University, Taigu 030031, China

[3]International Maize and Wheat Improvement Center (CIMMYT), Texcoco 56237, Mexico

*Corresponding authors: Chaonan Li, State Key Laboratory of Crop Gene Resources and Breeding, National Key Facility for Crop Gene Resources and Genetic Improvement, Institute of Crop Sciences, Chinese Academy of Agricultural Sciences, No. 12 Zhongguancun South St., Beijing 100081, China. Email: lichaonan@caas.cn; Ruilian Jing, State Key Laboratory of Crop Gene Resources and Breeding, National Key Facility for Crop Gene Resources and Genetic Improvement, Institute of Crop Sciences, Chinese Academy of Agricultural Sciences, No. 12 Zhongguancun South St., Beijing 100081, China. Email: jingruilian@caas.cn

‡These authors contributed equally to this work.

The author responsible for distribution of materials integral to the findings presented in this article in accordance with the policy described in the Instructions for Authors (https://academic.oup.com/plphys/pages/General-Instructions) is Chaonan Li.

Abstract

Root density, determined by root number, is a key trait for drought resistance and yield improvement. Here, we identified a drought-responsive root number regulator, TabHLH112-2A, in wheat (*Triticum aestivum*). Given its interaction with the essential factor of crown root initiation, TaMOR, TabHLH112-2A was subsequently designated TaMIP1. *mip1* mutants had fewer crown and lateral roots than the wild type (WT). TaMIP1 specifically bound to the E-box cis-element and induced the expression of genes involved in auxin and ABA signaling pathways, root development, and drought stress response. Two *TaMIP1* haplotypes were found in the natural population. Two nonsynonymous SNPs in the active domain led to enhanced transactivation activity of TaMIP1$^{Hap\text{-}2A\text{-}2}$, resulting in higher root dry weight. The *TaMIP1* and *TaMOR* haplotypes had additive effects on RDW, and the effect of *TaMOR* haplotypes was epistatic to that of *TaMIP1* haplotypes. Furthermore, *mip1* exhibited a lower survival rate under drought stress and a higher yield under well-watered conditions. Our findings elucidate the important roles of TaMIP1 in root density and the tradeoff between yield and drought resistance. The discovery of a regulatory module and combined haplotypes bring insights and genetic resources for drought resistance and high-yield breeding.

Introduction

Wheat is one of the major cereal crops, accounting for one-fifth of calories and proteins all over the world (Shewry and Hey 2015; Kumar et al. 2018). In recent years, due to climate change, abiotic stresses such as drought are increasingly affecting the growth and productivity of wheat (An et al. 2013; Budak et al. 2015; Norén et al. 2016). Roots are indispensable for plants to take up water and nutrients from soil, as well as to sense drought stress signals (Herder et al. 2010; Ye et al. 2018; Thorup-Kristensen et al. 2020). Optimal root system architecture is crucial for drought resistance and yield improvement in crops (Wasson et al. 2012; Lynch 2013; Li et al. 2021). Thus, mining key genes controlling root system architecture, elucidating the molecular mechanisms, and developing functional molecular markers will provide insight and potential targets for wheat breeding.

Monocot wheat has a fibrous root system, which consists of seminal roots, crown roots, and lateral roots. In contrast to the seminal roots, the crown roots and lateral roots are characterized by more number and stronger plasticity, which compose the major root system in wheat. They are indispensable for increasing root surface area for water and nutrient uptake. Given the vital roles, genes controlling crown root and lateral root development in crops have been studied. In rice, the LBD (LATERAL ORGAN BOUNDARIES DOMAIN) gene *CRL1* (*CROWN ROOTLESS 1*) acts downstream of ARF in the auxin signaling pathway to positively regulate the formation of crown and lateral roots (Inukai et al. 2005). Overexpression of the IAA-amido synthetase gene *OsGH3-2* (*GLYCOSIDE HYDROLASE 3-2*) exhibited few crown roots and hypersensitive to drought stress (Du et al. 2012). Root-specific overexpression of the NAC (NAM, ATAF1/2, and CUC2) gene

Received: September 28, 2025. **Accepted:** February 21, 2026

OsNAC6 caused increased root number and diameter and improved yield and drought tolerance (Lee et al. 2017). The R2R3-type MYB protein RRS1 (ROBUST ROOT SYSTEM 1) directly activates the expression of *OsIAA3* (*AUXIN/INDOLE-3-ACETIC ACID 3*) to repress lateral root formation and growth as well as drought tolerance (Gao et al. 2023). Maize bZIP (BASIC LEUCINE ZIPPER) transcription factor ZmbZIP4 targets genes related to stress response and root development to positively regulate primary root length and lateral root number and confer tolerance to drought and salt stress (Ma et al. 2018). In recent years, genes regulating root number in wheat and their functions in stress tolerance and yield have been gradually identified. The LBD protein TaMOR (MORE ROOT) is responsible for the crown and lateral root formation by regulating *PIN2* (*PIN-FORMED2*) expression. Its overexpression lines in rice showed increased root number and yield, while the gene knockout in wheat dramatically decreased the root number and yield (Li et al. 2022). The Tryptophan Aminotransferase gene *TaTAR2.1* (*TRYPTOPHAN AMINOTRANSFERASE RELATED 2.1*) in auxin biosynthesis pathway is essential for the formation and growth of lateral roots and yield increase of wheat (Shao et al. 2017). The KNAT3 (KNOTTED1-LIKE HOMEBOX GENE 3) homolog gene *LRD* (*LATERAL ROOT DENSITY*) represses lateral root growth and density under water stress in a GA-dependent pathway and negatively affects grain size and number (Placido et al. 2020). The drought responsive gene *TaSNAC8-6A* (*STRESS-RESPONSIVE NAC TRANSCRIPTION FACTOR 8-6A*) stimulates lateral root development and drought tolerance through regulating auxin and drought responsive genes (Mao et al. 2020).

The bHLH (BASIC HELIX-LOOP-HELIX) transcription factor family, one of the largest transcription factor families in plants, is widely present in eukaryotes. Its characteristic is the presence of a highly conserved bHLH domain consisting of 50 to 60 amino acid residues, which consists of a DNA binding domain composed of 10 to 15 amino acid residues and a helix-loop-helix domain (Castilhos et al. 2015). The core sequence recognized by bHLH proteins is E-box (5′-CANNTG-3′). bHLH genes are enriched in wheat genome (Guo and Wang 2017; Wei and Chen 2018). The wheat bHLH transcription factor TaAKS1 (ABA-RESPONSIVE KINASE SUBSTRATE 1) interacts with ethylene responsive factor TaERF87 (ETHYLENE-RESPONSE FACTOR 87) to synergistically activate the expression of proline biosynthesis genes *TaP5CS1* (*Δ-1-PYRROLINE-5-CARBOXYLATE SYNTHETASE 1*) and *TaP5CR1* (*Δ-1-PYRROLINE-5-CARBOXYLATE REDUCTASE 1*), which enhances drought tolerance through proline accumulation (Du et al. 2023). TabHLH27, orchestrating root growth and drought tolerance by interacting with different partners, acts as a positive regulator of root growth, yield, and water use efficiency (Wang et al. 2024). The ectopic expression of *TabHLH123* in rice leads to more roots by regulating the expression of genes related to crown root development, auxin metabolism, response, and transport (Wang et al. 2023). TabHLH49 directly upregulates the expression of dehydrin gene *WZY2* (*WHEAT ZHENGYIN 1 DEHYDRIN 2*) and improves drought tolerance of wheat (Liu et al. 2020). Thus, bHLH transcription factors play important roles in root development, drought resistance, and yield.

In this study, based on the phenotypic and transcriptomic analysis of the drought-resistant cultivar Jinmai 47, *TabHLH112-2A* associated with root dry weight (RDW) was selected as a candidate gene regulating root development in response to drought stress. TabHLH112-2A interacts with the key root number regulator TaMOR, so it was named as TaMIP1 (TaMOR interacting protein 1). Phenotypic analysis of *mip1* mutants and further molecular assays demonstrated that TaMIP1 integrates auxin and ABA signaling pathways to control root development. We further found the elite allelic variation of *TaMIP1* for RDW and the combined haplotype of *TaMIP1* and *TaMOR* resolving the trade-off between yield and drought resistance. These findings not only elucidate the molecular mechanism of *TaMIP1* but also provide potential targets for wheat genetic improvement of drought resistance and yield.

Results

TabHLH112-2A is the candidate gene regulating root development in response to drought stress

To explore bHLH genes involved in root development in response to drought stress, root phenotypes and transcriptomic data of the wheat cultivar Jinmai 47 under drought conditions were analyzed. The total root length, maximum root length, and lateral root number were inhibited by PEG-mimic drought treatment (Fig. 1a and 1b). Compared with control, 45 bHLH genes were differentially expressed in the root under PEG treatment (Fig. S1a). The expression pattern of the 45 bHLH genes in tissues showed that *TraesCS2A02G484700* and *TraesCS2B02G510800* were highly expressed in root but lowly or not expressed in other tissues (Fig. 1c), indicating their specific roles in root development.

TraesCS2A02G484700 and *TraesCS2B02G510800* are homologous genes, *TabHLH112-2A* and *TabHLH112-2B*. The open reading frames of *TabHLH112-2A*, *TabHLH112-2B*, and *TabHLH112-2D* are 2369, 2481, and 2577 bp, encoding 435, 444, and 443 amino acids, respectively (http://wheatomics.sdau.edu.cn/) (Fig. S1b). There is a highly conserved HLH domain in all 3 proteins. The similarity of TabHLH112-2A and TabHLH112-2B is 94.83%, that of TabHLH112-2A and TabHLH112-2D is 95.06%, and that of TabHLH112-2B and TabHLH112-2D is 95.96% (Fig. S1c). Phylogenetic analysis revealed that *TabHLH112*s are highly conserved in Triticeae (Fig. S1d).

In addition, genomic sequence polymorphisms of *TabHLH112 s* and association between genotypes and phenotypes were analyzed. Four SNPs were detected in *TabHLH112-2A* and 2 haplotypes were identified as shown in Fig. 1d. Among the 4 SNPs, 3 SNPs at 190, 807, and 1210 bp (SNP-190, SNP-807, and SNP-1210) are located in the exon. SNP-190 (T/C) and SNP-807 (C/T) caused changes in amino acids (V/A and P/L), and SNP-1210 is a synonymous SNP. Based on SNP-807, a dCAPS marker was developed for association analysis between genotypes and phenotypes of Population 2 (Fig. 1e). It was found that the SNPs of *TabHLH112-2A* were significantly associated with root dry weight at grain-filling stage (Table S1). Compared with *Hap*-2A-1 genotype, *Hap*-2A-2 genotype had higher root dry weight (Fig. 1f). There are 2 SNPs in the promoter of *TabHLH112-2B* associated with spikelet number per spike, but not with root phenotypes (Fan et al. 2024), and no SNP was detected in *TabHLH112-2D*. Thus, *TabHLH112-2A* was selected as the candidate gene regulating root development for further study.

TabHLH112-2A encodes a nuclear-localized protein interacting with TaMOR

In root, expression of *TabHLH112-2A* was repressed by PEG treatment but induced by auxin (IAA) and ABA treatments (Fig. 2a), indicating that *TabHLH112-2A* is involved in the auxin and ABA signaling pathways and response to drought stress. To clarify the subcellular localization of TabHLH112-2A, we constructed 35S: TabHLH112-2A-GFP

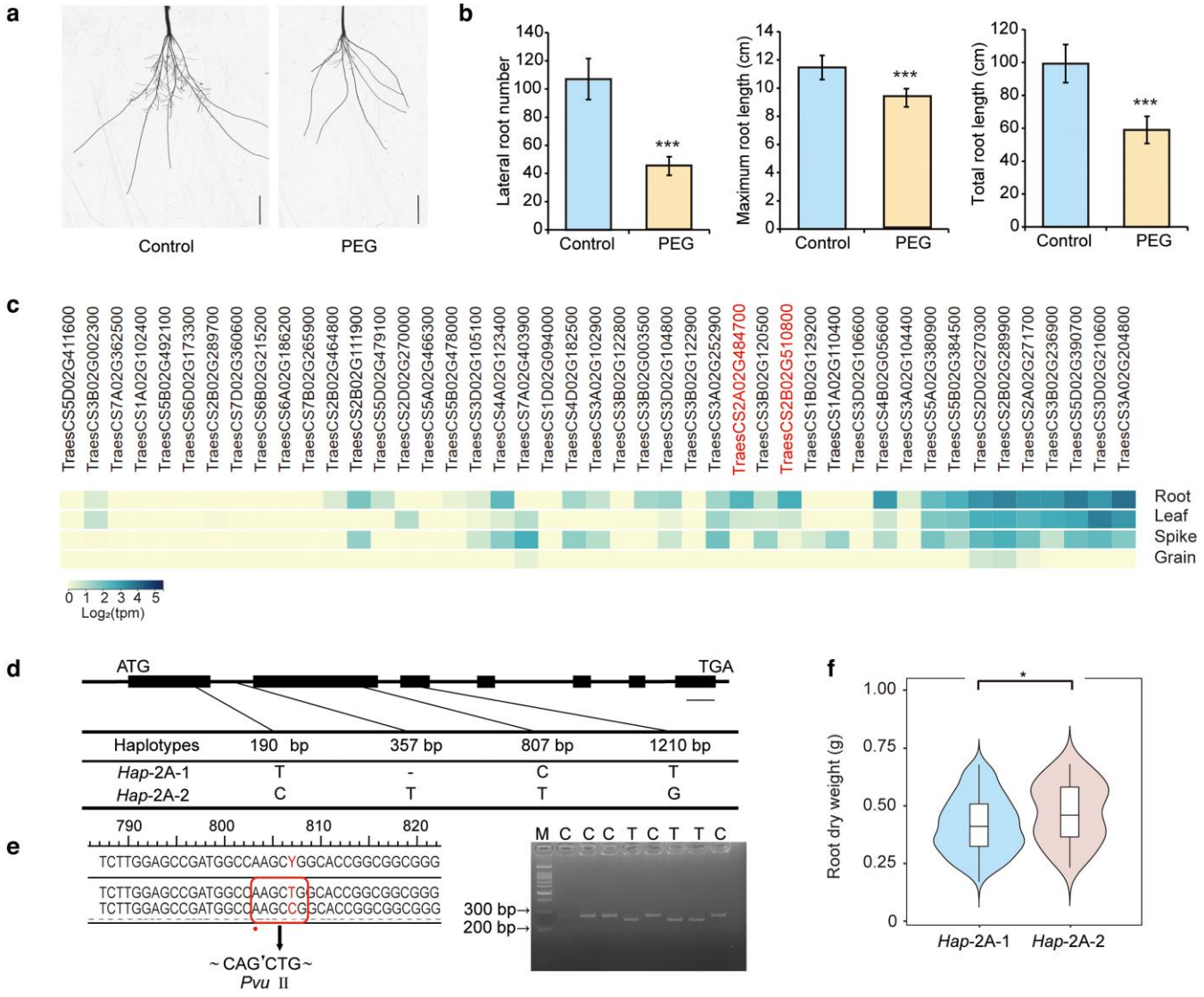

Figure 1 *TabHLH112-2A* is a drought-responsive gene associated with root dry weight. a) Roots of Jinmai 47 seedlings treated by PEG (polyethylene glycol) and control. Bars, 2 cm. b) Comparison of lateral root number, maximum root length, and total root length of Jinmai 47 seedlings treated by PEG and control. Values are means ± SD (n = 16). ***, $P < 0.001$. c) The expression patterns of the bHLH genes among differentially expressed genes. d) Sequence polymorphisms of *TabHLH112-2A* coding sequence detected in Population 1. Bar, 100 bp. e) Development of molecular marker based on SNP-807. SNP, mismatched base and restriction site are marked with the red letter, red dot and box, respectively. M, 100 bp DNA ladder. C, *Hap*-2A-1; T, *Hap*-2A-2. f) Root dry weight comparison at grain-filling stage of 2 haplotypes. The central line represents the median; The box limits indicate the upper (75th) and lower (25th) quartiles; The whiskers extend to the furthest data points within 1.5 times the interquartile range (IQR). *, $P < 0.05$. Student *t* test was used to determine the statistical significance between different groups.

and transiently expressed in *N. benthamiana* leaves. It was found that the GFP signal merged with the signal of nuclear marker, indicating that TabHLH112-2A is localized in the nucleus (Fig. 2b). Furthermore, we detected its transactivation activity using the yeast system. The full-length CDS and truncated fragments according to the position of bHLH domain (308 to 357 aa) were fused with BD. As shown in Fig. 2c, BD-TabHLH112-2A (1 to 435 aa) and BD-TabHLH112-2A-1 (1 to 307 aa) grew normally on SD-Trp/Leu/His/Ade medium, indicating that TabHLH112-2A has transactivation activity through the fragment TabHLH112-2A-1.

We screened the partners of TabHLH112-2A by yeast 2-hybrid screening assay. The key regulator of root number, TaMOR, was identified as a candidate interacting protein. To test the interaction between TabHLH112-2A and TaMOR, we performed yeast 2-hybrid assay. TaMOR210 (1 to 210 aa) without transactivation activity constructed into vector pGBKT7 was used in the assay (Li et al. 2022). The results showed that TabHLH112-2A interacts with TaMOR in yeast (Fig. 2d). Furthermore, we conducted luciferase complementation imaging (LCI), biomolecular fluorescence complementation (BiFC), and co-immunoprecipitation (Co-IP) assays to confirm their interaction in vivo. Strong luciferase activity was detected when TaMOR-nLUC and cLUC-TabHLH112-2A were coexpressed in LCI assay (Fig. 2e). The results of BiFC displayed that when TaMOR-YNE and TabHLH112-2A-YCE were coexpressed yellow fluorescent protein (YFP) fluorescence signal was observed in the nucleus (Fig. 2f). And TabHLH112-2A-Flag was co-immunoprecipitated with TaMOR-GFP, but

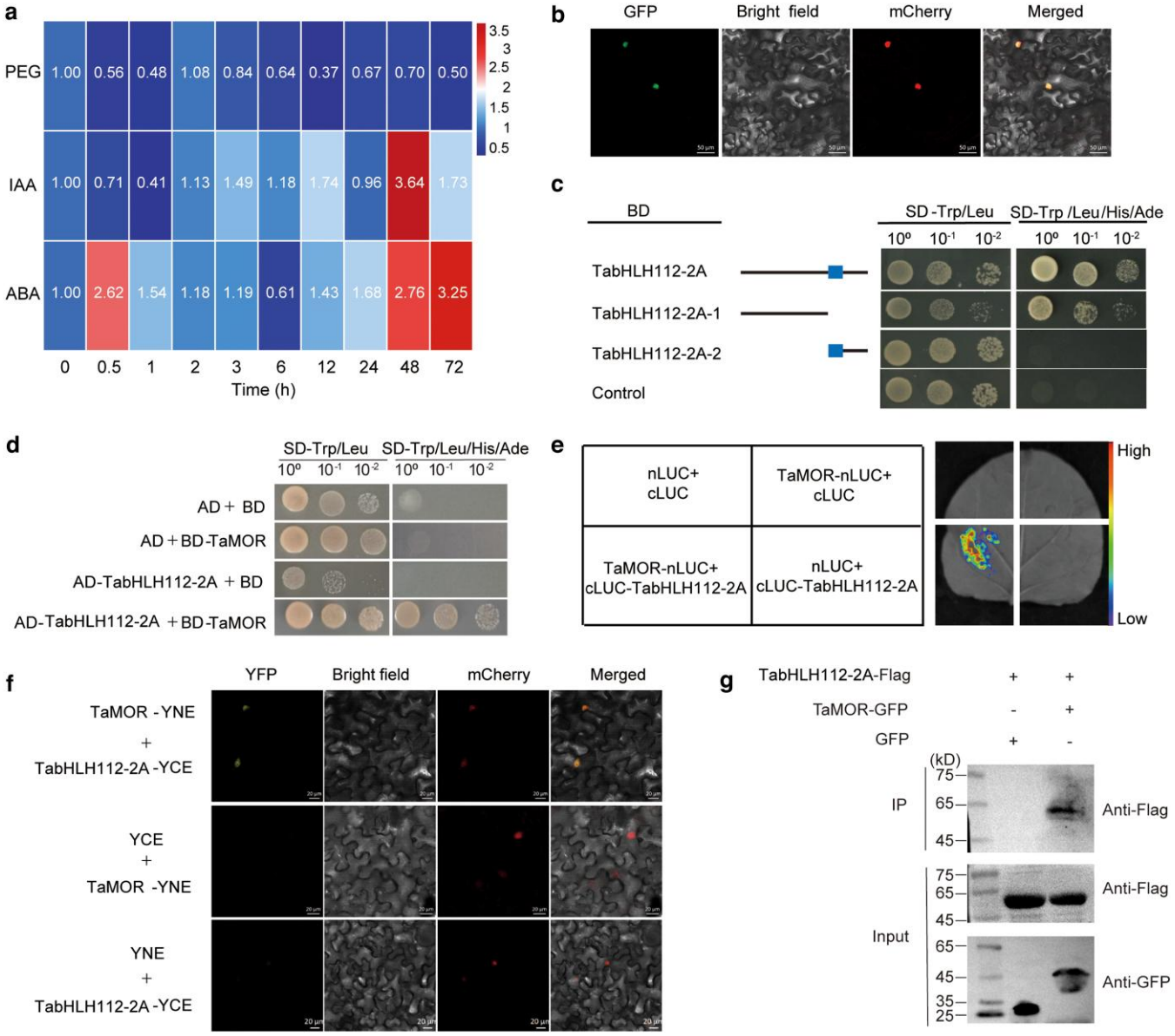

Figure 2 The nuclear-localized TabHLH112-2A interacts with TaMOR. a) Expression patterns of *TabHLH112* under 16.1% PEG, 0.1 mM IAA (indole-3-acetic acid), and 50 μM ABA (Abscisic acid) treatment. The values and the color in each box represent the fold changes of *TabHLH112-2A* expression levels relative to 0 h. b) Subcellular localization of TabHLH112-2A in *N. benthamiana* leaves. H2B-mCherry was used as a nucleus marker. Bars, 50 μm. c) Transactivation activity of the full-length and truncated TabHLH112-2A. The full-length TabHLH112-2A (1 to 435 aa) and truncated fragments TabHLH112-2A-1 (1-307 aa) and TabHLH112-2A-2 (308 to 435 aa) were fused with BD (Binding domain) of pGBKT7 and co-transformed with pGADT7 into yeast. The control was yeast transformed with pGBKT7 and pGADT7. Blue box represents the HLH domain. d) TabHLH112-2A interacts with TaMOR in yeast. e) The interaction of TabHLH112-2A and TaMOR detected by LCI assays in *N. benthamiana*. f) BiFC assays showed TabHLH112-2A interacts with TaMOR in nucleus of *N. benthamiana*. H2B-mCherry was used as a nucleus marker. Bars, 20 μm. g) Co-IP assays showed TabHLH112-2A interacts with TaMOR in *N. benthamiana*. –, absence of proteins; +, presence of proteins.

not with GFP in the CoIP assays (Fig. 2g). Therefore, TabHLH112-2A was designated as TaMIP1 (TaMOR-interacting protein 1).

TaMIP1 increases the number of crown roots and lateral roots

To understand the effect of *TaMIP1* on root development, we generated mutants by CRISPR-Cas9 editing technology targeting *TaMIP1* in all 3 genomes. Three independent homozygous mutants with different edits, *mip1-1*, *mip1-2*, and *mip1-6*, were identified for further study (Fig. 3a). There was no significant difference in seminal root number, crown root number, and maximum root length between the *mip1* mutants and wild type (WT), but the *mip1* mutants had fewer lateral roots than WT at 10-d-old seedling stage (Fig. 3b and 3c; Fig. S2a). Methylene blue staining assay showed that the lateral root primordium number was decreased when *TaMIP1* was mutated (Fig. 3d and 3e). The results demonstrated that *TaMIP1* positively regulates lateral root formation at seedling stage.

We further analyzed the root phenotypes of plants in pipes and field at booting stage and grain-filling stage. At booting stage, pipe

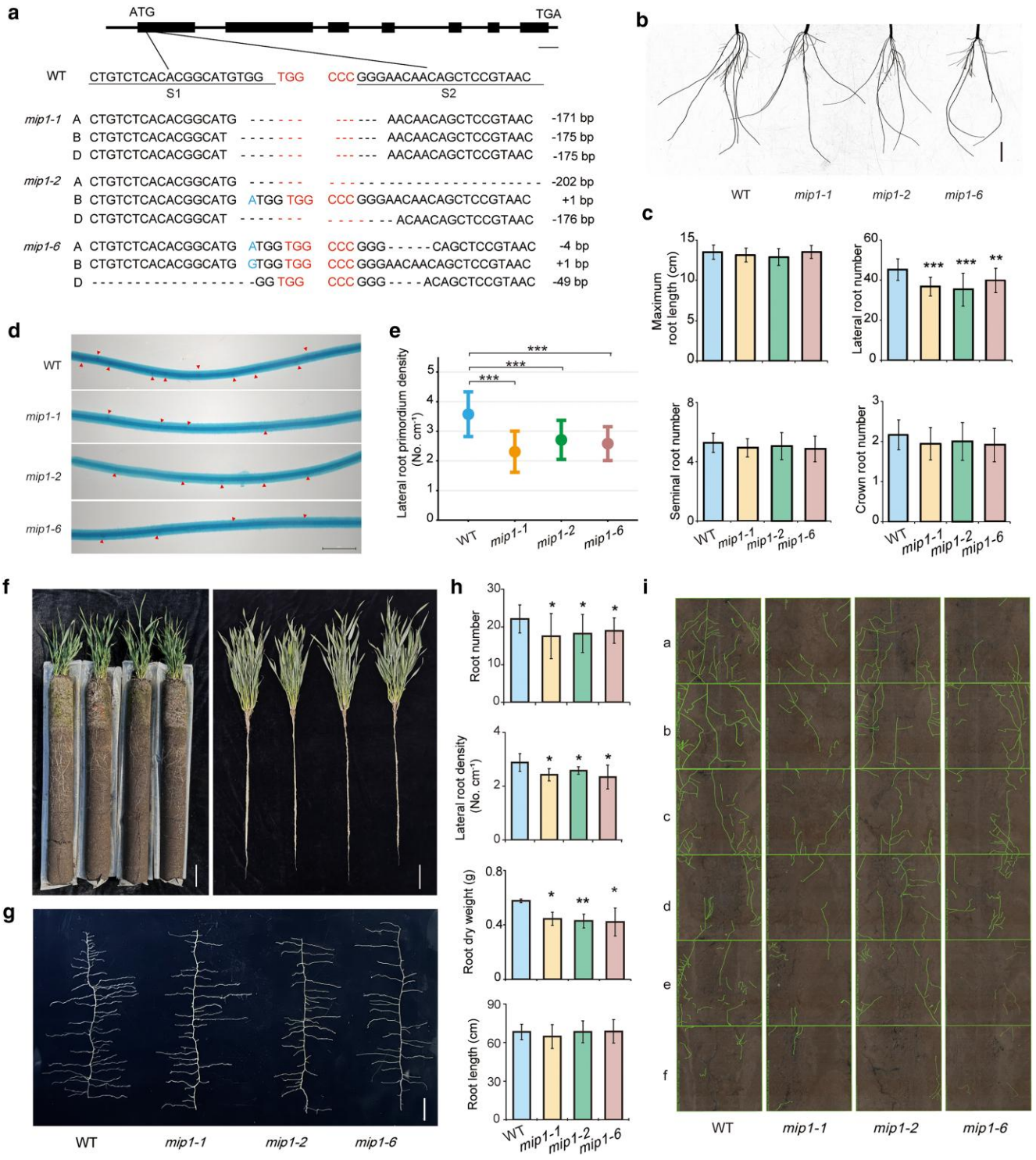

Figure 3 Root phenotypes of *TaMIP1* mutants at seedling stage and booting stage. a) Identification of *TaMIP1* homozygous mutants generated by CRISPR/Cas9 technology. The black boxes represent exons, and the black lines represent introns. The target sequences are indicated as S1 and S2, and PAMs (protospacer adjacent motif) are noted in red. The blue letters represent the inserted bases; the short lines represent deletion of corresponding sequences. Bar, 100 bp. b) Roots of 10-d-old WT (wild type) and *mip1* mutants seedlings. Bar, 2 cm. c) Comparisons of maximum root length, lateral root number, seminal root number, and crown root number between 10-d-old WT and mutants. Values are means ± SD (n = 18). **, $P < 0.01$; ***, $P < 0.001$. d) Lateral root primordia of WT and *mip1* mutants. Roots at a distance of 2 to 4 cm from the root tip were sampled for methylene blue staining. The red arrow indicates the lateral root primordium. Bar, 2 mm. e) Comparison of lateral root primordium number of WT and mutants. Values are means ± SD (n = 13). ***, $P < 0.001$. f) Phenotypes of WT and *mip1* mutants at booting stage. Bars, 10 cm. g) Lateral root distribution of the truncated root. Bar, 2 cm. h) Comparisons of root number, root dry weight, lateral root density and root length between WT and mutants at booting stage. Values are means ± SD (n = 9). *, $P < 0.05$; **, $P < 0.01$. i) Minirhizotron images of WT and *mip1* mutants in field at booting stage. a-f, soil layers of different depths. a, 0 to 14.1 cm; b, 14.1 to 28.3 cm; c, 28.3 to 42.4 cm; d, 42.4 to 56.6 cm; e, 56.6 to 70.7 cm; f, 70.7 to 84.8 cm. Student *t* test was used to determine the statistical significance between different groups.

assays and field minirhizotron images showed that *mip1* mutants exhibited decreased root distribution in soil compared with WT (Fig. 3f, 3h, and 3i). The roots in pipes 10 to 25 cm away from the root tip were truncated and washed, and then average lateral root number per centimeter of every root was counted to investigate the lateral root density. The root number, root dry weight, and lateral root density were significantly reduced, but the root length did not change significantly when *TaMIP1* was mutated (Fig. 3g and 3h). At grain-filling stage, the root number and root dry weight of *mip1* mutants were significantly lower than those of WT (Fig. S2b and S2c), which is consistent with the phenotype at the booting stage. Taken together, *TaMIP1* promotes crown root and lateral root development in wheat.

To determine whether the function of *TaMIP1* is conservative in other monotcots, homozygous overexpression lines of *TaMIP1* in rice were obtained (OE-12 and OE-20) (Fig. S3c). Compared with WT, the root number and root dry weight increased of overexpression rice lines, but the root length and tiller number did not show significant changes at 1-mo-old seedling stage and booting stage (Fig. S3a-3e). Expression of genes controlling crown root development, *OsCRL1*, *OsCRL5*, *OsMADS50*, and *OsSPL12* (*SQUAMOSA PROMOTER BINDING PROTEIN-LIKE 12*) (Inukai et al. 2005; Kitomi et al. 2011; Shao et al. 2019), was detected. The expression of the positive regulator *OsCRL5* was induced, while the expression of negative regulators *OsMADS50* and *OsSPL12* was repressed when *TaMIP1* was overexpressed (Fig. S3f). Therefore, the positive regulatory effect of *TaMIP1* on root number is conserved in rice and wheat.

The expression of genes involved in auxin and ABA signaling pathways, drought response, and root development is regulated by TaMIP1

To further analyze the function of *TaMIP1* on root development, we carried out RNA-seq to identify differentially expressed genes (DEGs) in roots of the mutant *mip1-6* and WT at the booting stage. Compared with WT, 1989 upregulated genes and 4516 downregulated genes were detected in *mip1-6* (Fig. S4a). KEGG analysis showed that the DEGs were enriched in metabolic pathway and plant hormone signal transduction (Fig. S4b). Among these DEGs, genes involved in auxin synthesis, transport, and signal transduction pathway, such as *PIN3a*, *ARF11* (*AUXIN RESPONSE FACTOR 11*), and *YUC11* (*YUCCA 11*), and genes involved in root development, such as *LBD*s, *SCR1* (*SCARECROW1*), and *GATA*s (*GATA-BINDING FACTOR*) and *SHR1* (*SHORT ROOT 1*), were downregulated in the *mip1-6* (Fig. 5a; Fig. S4c). Meanwhile, ABA- and drought stress–responsive genes, such as *LEA1* (*LATE EMBRYOGENESIS ABUNDANT 1*) (Wang et al. 2007; Olvera-Carrillo et al. 2011), *DHN2* (*DEHYDRIN 2*) (Riyazuddin et al. 2022), *DREB3* (*DEHYDRATION RESPONSIVE ELEMENT-BINDING 3*) (Shavrukov et al. 2016), and *PYL4* (*PYRABACTIN RESISTANCE 1-LIKE 4*) (Usman et al. 2020; Mao et al. 2022), were strongly repressed in *mip1* mutants (Fig. 5b; Fig. S4d), indicating that *TaMIP1* is involved in auxin and ABA signaling pathways, drought response, and root development.

To reveal the mechanism of TaMOR-TaMIP1 regulating root development, Venn diagrams of DEGs between WT and *mip1-6* between control and *mor-6* (Li et al. 2022) were analyzed. It was found that 529 genes were commonly upregulated and 1211 genes were downregulated in both *mip1-6* and *mor-6*, while 1460 upregulated genes and 3305 downregulated genes were specifically observed in *mip1-6* mutants (Fig. 5c and 5d). Among them, expression of genes such as *GATA2*, *BRN2* (*BEARSKIN 2*), *YUC9*, and *IAA31* was repressed in both *mip1-6* and *mor-6* (Fig. 5e and 5g; Fig. S5a), while expression of genes such as *AHL20* (*AT-HOOK MOTIF NUCLEAR LOCALIZED 20*), *LBD13*, *SHR1*, and *SAU76* (*SMALL AUXIN-UPREGULATED RNA 76*) was repressed in *mip1-6* but unchanged in *mor-6* (Fig. 5f and 5h; Fig. S5b). Therefore, TaMIP1 regulates expression of genes involved in auxin signaling pathway and root development in the TaMOR-TaMIP1 module and TaMOR-independent pathway.

TaMIP1 directly induces target gene expression through specifically binding of E-box

To detect the direct targets of TaMIP1, we selected genes controlling root development that were significantly downregulated in *mip1-6* as candidate genes to conduct yeast 1-hybrid assays. The result indicated that TaMIP1 can bind to the promoters of *LBD13*, *SHR1*, *LBD15*, *BRN2*, *GATA4*, and *SCR1* (Fig. 6a). bHLH proteins are known to bind to the E-box (5′-CANNTG-3′) in the promoters of downstream genes. Based on the result of yeast 1-hybrid assays, 3 E-box sequences, CATATG, CAATTG, and CAGTTG were predicted as the binding sites of TaMIP1, which also existed in the promoters of *DREB3* and *PYL4* (Fig. S6a and S6b). To verify the prediction, EMSA was performed with probes containing the predicted binding sequences. GST-TaMIP1 could bind to the probes, and the bindings were suppressed by cold probes (Fig. 6b), indicating that TaMIP1 specifically binds to the CATATG, CAATTG, and CAGTTG sequences in the promoters of target genes to participate in the auxin and ABA signaling pathways, drought response and root development.

Given that TaMOR interacts with TaMIP1, the question whether TaMOR binds to the targets of TaMIP1 was raised. Yeast 1-hybrid assays were performed to detect the bindings of TaMOR and the promoters of target genes. The result showed that only *BRN2* is bound by TaMOR (Fig. 6c). LBD genes were enriched in the DEGs of WT vs *mip1-6*. *TaMOR* encodes a LBD protein, and its promoter has a CATATG E-box in the P2 fragment (Fig. 6e). We examined whether *TaMOR* was directly regulated by TaMIP1 using RT-qPCR and yeast 1-hybrid assay. The expression of *TaMOR* in *mip1* was significantly reduced compared with WT, while there was no significant change of *TaMIP1* expression in control and *mor-6*, indicating that expression of *TaMOR* is regulated by TaMIP1 (Fig. 6d). The result of yeast 1-hybrid assay showed that TaMIP1 binds to the P2 fragment of *TaMOR* promoter, and TaMOR can bind to the promoter of itself (Fig. 6e).

To investigate the effects of TaMOR-TaMIP1 module on expression of targets, dual luciferase reporter assays were conducted. The promoters of target genes were fused with *LUC* gene as reporters. TaMIP1-GFP and TaMOR-GFP were effectors. For the reporters *proBRN2*:LUC and *proTaMOR*:LUC, LUC activity was induced when TaMIP1-GFP or TaMOR-GFP was expressed alone and increased to a higher level when TaMIP1-GFP and TaMOR-GFP were coexpressed (Fig. 6f). Previous studies revealed that TaMOR interacts with ARF5 to directly induce *PIN2* expression (Li et al. 2022). We further investigated the interaction of TaMIP1 and ARF5 and its regulation of *PIN2* expression. The results indicated that TaMIP1 does not interact with ARF5, but it can bind to the P2 of *PIN2* promoter to induce *PIN2* expression (Fig. S6c-e; Fig. 5g). Hence, the coexpression of TaMOR and TaMIP1 had additive effects on inducing *BRN2*, *PIN2*, and *TaMOR* expression.

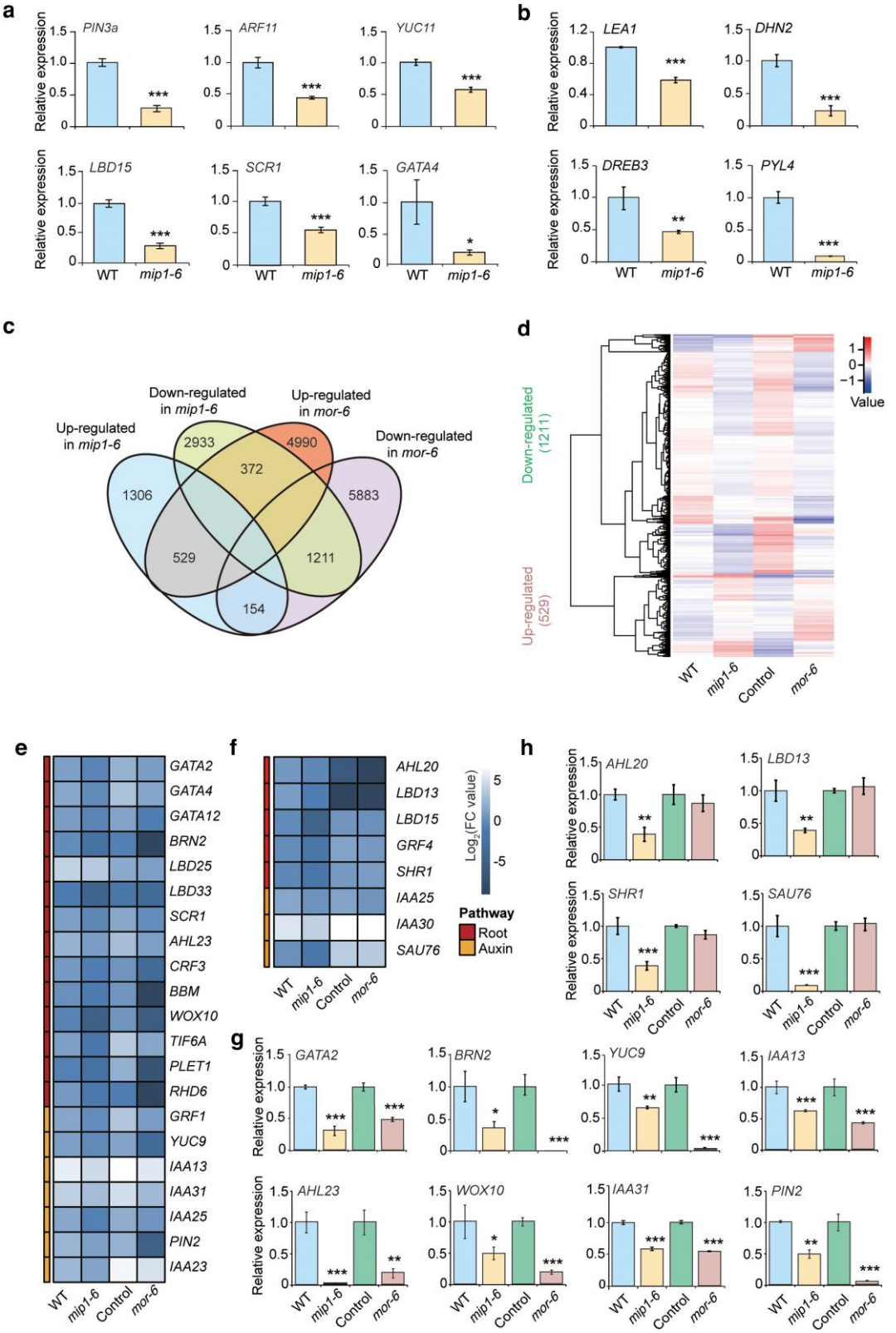

Figure 4 Transcriptomic analysis of WT and *mip1-6*. a) The expression of root development and auxin signaling genes in WT and *mip1-6*. Values are means ± SD (n = 3). b) The expression of drought-responsive and ABA signaling genes in *mip1-6* and WT. Values are means ± SD (n = 3). c) Venn diagrams of differentially expressed genes in WT vs *mip1-6* and control vs *mor-6*. d) Upregulated and downregulated genes in both *mip1-6* and *mor-6*. e) Downregulated genes in both *mip1-6* and *mor-6*. f) Down-regulated in *mip1-6* but unchanged in *mor-6*. The red box represents root development, and the yellow box represents auxin signaling pathway. g) RT-qPCR validation of downregulated genes in *mip1-6* and *mor-6*. Values are means ± SD (n = 3). h) Validation of downregulated genes in *mip1-6* but unchanged in *mor-6*. Values are means ± SD (n = 3). Student *t* test was used to determine the statistical significance between different groups. *, $P < 0.05$; **, $P < 0.01$; ***, $P < 0.001$.

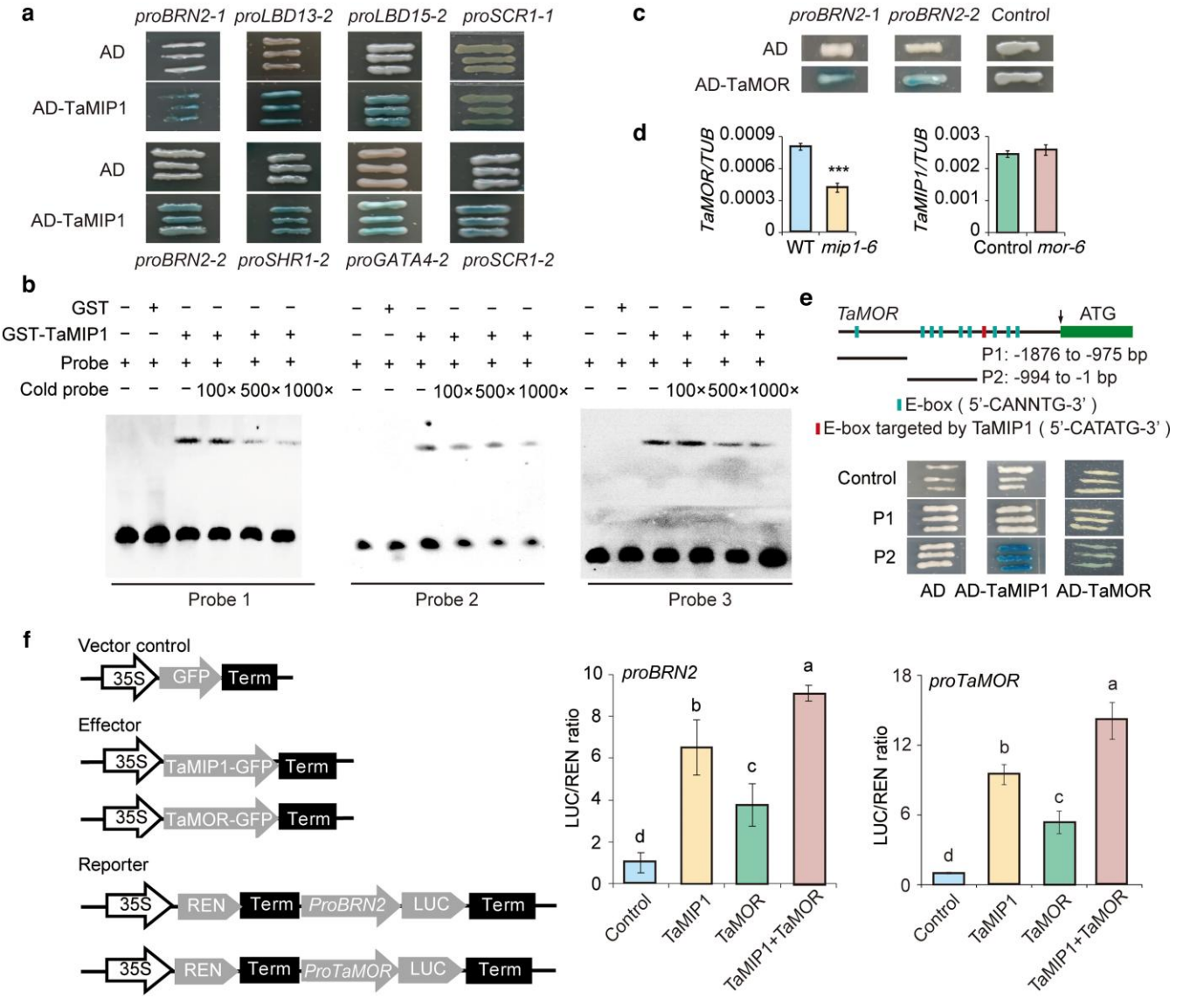

Figure 5 TaMIP1 directly induces expression of target genes by binding to the specific E-box sequences. a) TaMIP1 binds to promoters of *LBD13*, *SHR1*, *LBD15*, *BRN2*, *GATA4*, and *SCR1* in yeast. Two fragments (−1, −2000 ~ −1000 bp; −2, −1000 ~ −1 bp) of each promoter were constructed into pLacZi vector. TaMIP1 was fused with AD of pB42AD. b) TaMIP1 specifically binds to the E-box sequences CATATG, CAATTG and CAGTTG. Probe, biotin-labeled probe. Cold probe, unlabeled probe. −, absence of proteins or probes. +, presence of proteins or probes. 100×, 500×, 1000×, the concentration of cold probe is 100 times, 500 times, and 1000 times of probe, separately. Probe 1, sequence containing the E-box CATATG. Probe 2, sequence containing the E-box CAATTG. Probe 3, sequence containing the E-box CAGTTG. c) TaMOR binds to *BRN2* promoter in yeast. d) Expression of *TaMOR* in WT and *mip1-6*, and expression of *TaMIP1* in control and *mor-6*. Values are means ± SD (n = 3). ***, $P < 0.001$. e) TaMIP1 and TaMOR binds to P2 fragment of TaMOR promoter in yeast. Blue rectangles represent the E-boxes, and the red rectangle represents the E-box bound by TaMIP1. f) Induction of *BRN2* and *TaMOR* expression by TaMIP1, TaMOR and TaMOR-TaMIP1 module. Values are means ± SD (n = 3). Lowercase letters indicate significant differences between groups ($P < 0.05$). Student *t* test was used to determine the statistical significance between different groups.

TaMIP1 controls the trade-off between yield potential and drought resistance

Crown roots and lateral roots of monocots are responsible for increasing the surface area to absorb more water to cope with drought stress (Comas et al. 2013), but trade-off exists between the underground growth and yield (Fradgley et al. 2020). To investigate the function of *TaMIP1* in drought resistance and yield potential, we first detected the survival rates of *mip1* mutants and WT under drought stress at seedling stage. The leaves of mutants exhibited significant wilting compared with WT under drought stress (Fig. 4a). After 18 d of drought treatment and 3 d of rewatering, the survival rate of WT was significantly higher than that of *mip1* (Fig. 4b and 4c), suggesting that *TaMIP1* is responsible for wheat drought resistance at seedling stage.

In addition, we observed and compared the phenotypes of *mip1* mutants and WT under conventional normal irrigation and water-saving irrigation conditions in the field. The results showed that under WW (Well-watered) conditions, *mip1* mutants exhibited increased spike length, spikelet number per spike, grain number per spike,

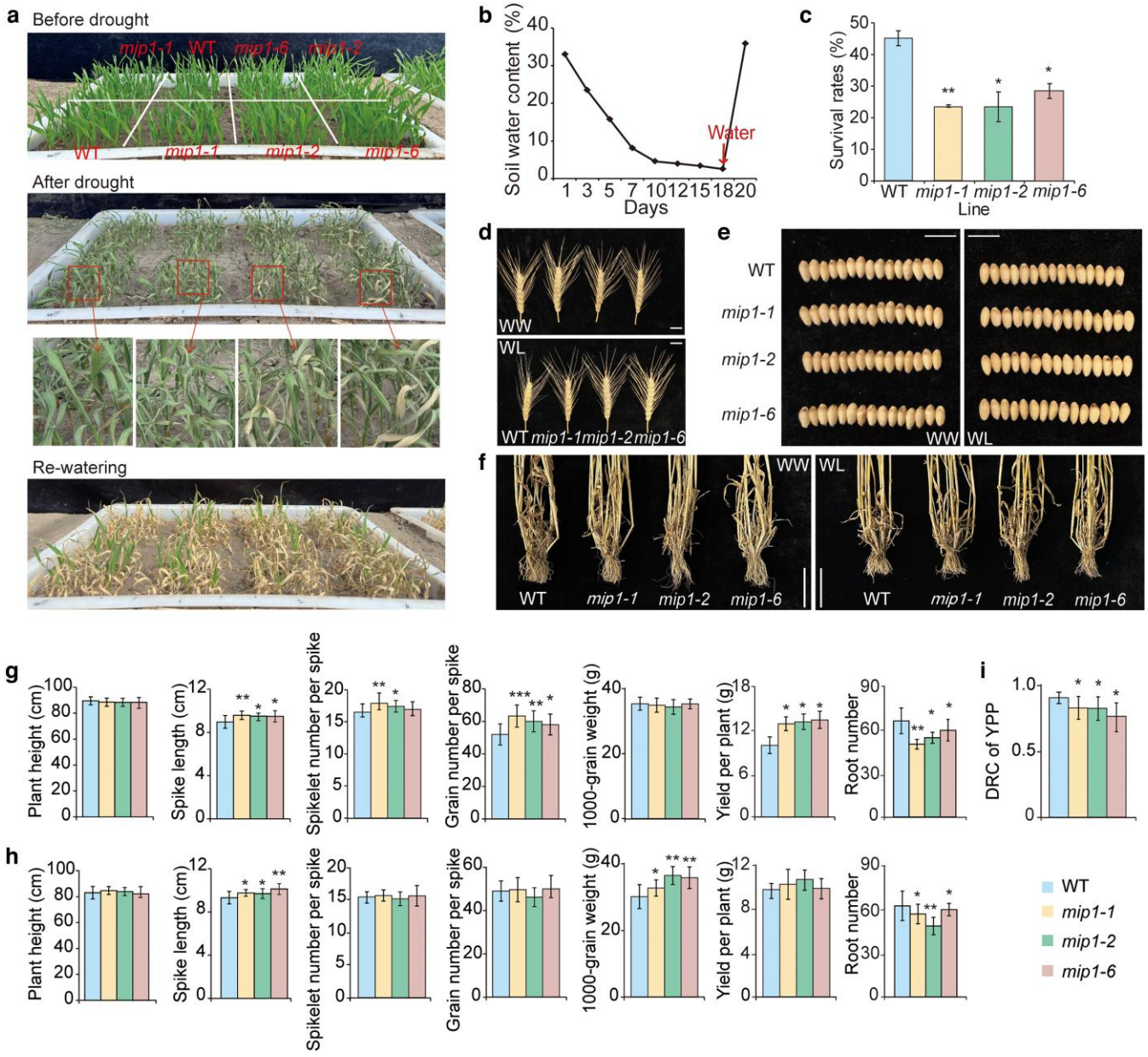

Figure 6 Phenotypes of WT and *mip1* mutants under WW and WL conditions. a) Phenotypes of WT and *mip1* mutants under drought stress at seedling stage. The seedlings at 3-leaf stage were treated by drought for 18 d, and then rewatering. b) The soil water content during the period of drought treatment and rewatering. Values are means ± SD (n = 3). c) Survival rates of WT and *mip1* mutants after drought treatment and rewatering. Values are means ± SD (n = 4). d) Spikes of WT and *mip1* mutants under WW and WL conditions. Bars, 3 cm. e) Grains of WT and *mip1* mutants under WW and WL conditions. Bars, 1 cm. f) Root number phenotype of WT and *mip1* mutants under WW and WL conditions. g, h) Bars, 10 cm. Statistical data of phenotypes under WW (g) and WL (h) conditions. i) DRC of YPP (drought resistance coefficient of yield per plant) of WT and *mip1-6* mutants. Values are means ± SD (n = 16). Student *t* test was used to determine the statistical significance between different groups. *, $P < 0.05$; **, $P < 0.01$; ***, $P < 0.001$.

and yield per plant compared with WT. Under WL (Water-limited) conditions, the spike length and 1000-grain weight of *mip1* mutants were significantly increased, while the yield per plant was similar with WT (Fig. 4d-h). In addition, we found a significant decrease of root number in *mip1* mutants compared to WT at maturation stage (Fig. 6f-6h). The drought resistance coefficient of yield per plant of the mutants was significantly lower than WT (Fig. 4i). All the results illustrated that the positive regulator of root number, TaMIP1, controls the trade-off between yield potential and drought resistance.

The nonsynonymous SNPs associated with root dry weight affect the transactivation activity of TaMIP1

The root dry weight of the 2 haplotypes of *TaMIP1* is significantly different. Interestingly, both of the amino acids changed by the 2 nonsynonymous SNPs are located in the region with transactivation activity. Then we tested the transactivation activities of TaMIP1$^{Hap\text{-}2A\text{-}1}$ and TaMIP1$^{Hap\text{-}2A\text{-}2}$ and their binding to target genes in yeast. As shown in Fig. 7a and 7b, similar with TaMIP1$^{Hap\text{-}2A\text{-}1}$ (Fig. 2c and 6a), TaMIP1$^{Hap\text{-}2A\text{-}2}$ has transactivation activity, and can bind to target

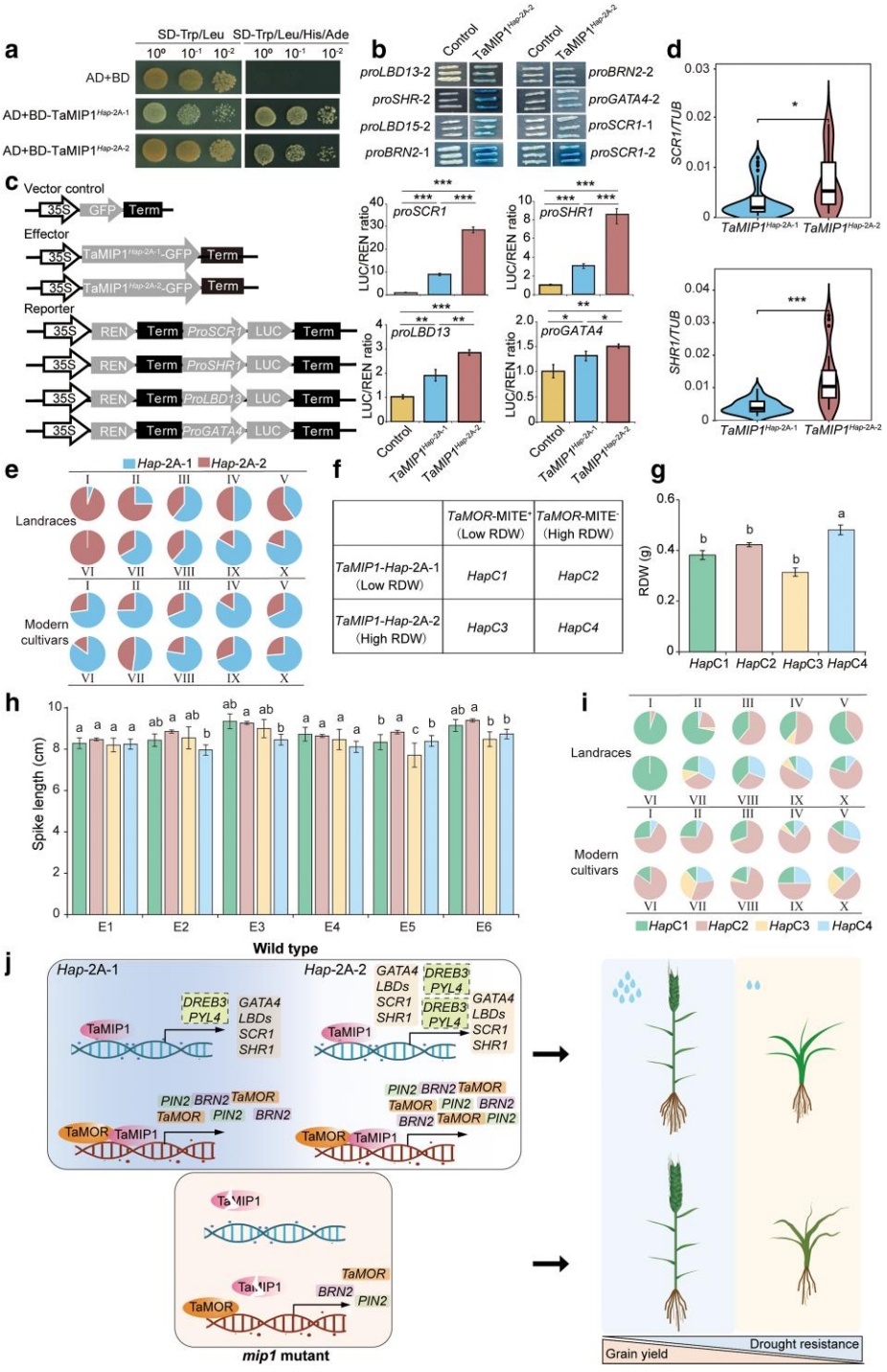

Figure 7 Function and frequency analysis of haplotypes. a) Transactivation activity of *TaMIP1* haplotypes in yeast. b) The binding of target genes by TaMIP1$^{Hap\text{-}2A\text{-}2}$ in yeast. c) The transactivation of target genes by TaMIP1$^{Hap\text{-}2A\text{-}1}$ and TaMIP1$^{Hap\text{-}2A\text{-}2}$. Values are means ± SD (n = 3). *, $P < 0.05$; **, $P < 0.01$; ***, $P < 0.001$. d) The expression of *SCR1* and *SHR1* in *TaMIP1* genotypes of the Population 2. The central line represents the median; The box limits indicate the upper (75th) and lower (25th) quartiles. The whiskers extend to the furthest data points within 1.5 times the interquartile range (IQR) (n = 51). *, $P < 0.05$; ***, $P < 0.001$. e) The frequency of *TaMIP1* haplotypes in landraces and modern cultivars in the 10 Chinese major wheat zones. I, Northern Winter Wheat Zone; II, Yellow and Huai River Valleys Facultative Wheat Zone; III, Middle and Low Yangtze Valleys Autumn-Sown Spring Wheat Zone; IV, Southwestern Autumn-Sown Spring Wheat Zone; V, Southern Autumn-Sown Spring Wheat Zone; VI, Northeastern Spring Wheat Zone; VII, Northern Spring Wheat Zone; VIII, Northwestern Spring Wheat Zone; IX, Qinghai-Tibetan Plateau Spring-Winter Wheat Zone; X, Xinjiang Winter-Spring Wheat Zone. f) The combination of *TaMIP1* and *TaMOR* haplotypes. g) RDW of *HapC1-C4* haplotypes in Population 2. Error bars represent ± SD. h) Spike length of *HapC1-C4* haplotypes in Population 2 in 6 environments. E1, 16-SY-DS; E2, 16-SY-WW; E3, 16-CP-WW; E4, 16-CP-DS; E5, 17-CP-DS; E6, 17-CP-WW. Abbreviations: CP, Changping; DS, drought stress; SY, Shunyi; WW, well-watered. Error bars represent ± SD. *HapC1* (n = 30), *HapC2* (n = 236), *HapC3* (n = 2), and *HapC4* (n = 41) are 4 combined haplotypes. Lowercase letters indicate significant differences between groups ($P < 0.05$). i) The frequency of *HapC1-C4* in landraces and modern cultivars. j) The working model of *TaMIP1* modulating root number and trade-off between drought resistance and grain yield. Student *t* test was used to determine the statistical significance between different groups.

genes. Furthermore, we performed dual-luciferase reporter assays using the reporters *proSCR1*:LUC, *proSHR1*:LUC, *proLBD13*:LUC, and *proGATA4*:LUC to test the transcriptional activation of target genes by 2 haplotypes. Expression of target genes were induced by TaMIP1$^{Hap\text{-}2A\text{-}1}$ and TaMIP1$^{Hap\text{-}2A\text{-}2}$, and the LUC signal was stronger when TaMIP1$^{Hap\text{-}2A\text{-}2}$ was coexpressed, indicating the transactivation activity of TaMIP1$^{Hap\text{-}2A\text{-}2}$ was significantly higher than that of TaMIP1$^{Hap\text{-}2A\text{-}1}$ (Fig. 7c). We further analyzed the expression levels of target genes in the genotypes with 2 haplotypes in Population 2, separately. The expression of target genes in *Hap*-2A-2 genotype was significantly higher than that in *Hap*-2A-1 genotype (Fig. 7d). These results suggested that the non-synonymous SNPs affect the transactivation activity of TaMIP1 and are responsible for the phenotypic differences between *Hap*-2A-1 and *Hap*-2A-2.

In addition to higher RDW, *Hap*-2A-2 has shorter spike than *Hap*-2A-1 (Fig. S7a). To determine the breeding selection of the 2 haplotypes, we tested the distribution in 10 major wheat zones in China, as well as in wheat breeding process. In 157 landraces, the presence of *Hap*-2A-1 and *Hap*-2A-2 was 45% versus 55%. While in 348 modern cultivars, the selection was toward *Hap*-2A-1 and its occurrence increased to 73%, and *Hap*-2A-2 only took up 27%. The frequency of *Hap*-2A-1 increased significantly in wheat regions except the arid and semi-arid climate regions of the Northern Spring Wheat Zone (VII), Qinghai-Tibetan Plateau Spring-Winter Wheat Zone (IX), and Xinjiang Winter-Spring Wheat Zone (X) (Fig. 7e). The frequency analysis of the 2 haplotypes from pre-1950 to 1990s showed that the proportion of *Hap*-2A-1 increased significantly in wheat breeding history, with corresponding increase in spike length and decrease in root dry weight (Fig. S7b and S7c). The results implied that the *Hap*-2A-1 genotype with longer spike has been generally positively selected along with the selection of yield-related traits, while the *Hap*-2A-2 genotype with higher root dry weight has been positively selected only in part of arid and semi-arid regions in Chinese wheat breeding.

TaMIP1 and *TaMOR* haplotypes have additive effects on RDW

TaMIP1-TaMOR module positively regulates root number, and TaMIP1 induces *TaMOR* expression by binding to its promoter, so we detected whether *TaMIP1* and *TaMOR* haplotypes have combined effects on RDW. According to the identified haplotypes of *TaMIP1* and *TaMOR* (Fig. 1d and 1f) (Li et al. 2022), 4 combinations were divided into low-/low– (*TaMIP1-Hap*-2A-1/*TaMOR-MITE*$^{+}$), low-/high– (*TaMIP1-Hap*-2A-1/*TaMOR*-MITE^{-}), high-/low– (*TaMIP1-Hap*-2A-2/*TaMOR*-MITE^{+}), and high-/high– (*TaMIP1-Hap*-2A-2/*TaMOR*-MITE^{-}) RDW haplotypes, named *HapC1-C4*, respectively (Fig. 7f). Among the 4 combined haplotypes, the RDW of *HapC4* (*TaMIP1-Hap*-2A-2/*TaMOR*-MITE^{-}) was the highest, indicating the additive effect of the *TaMIP1* and *TaMOR* haplotypes with high RDW. The RDW of *HapC1* (low-*TaMIP1*/low-*TaMOR*) and *HapC3* (high-*TaMIP1*/low-*TaMOR*) was lower than *HapC2* (low-*TaMIP1*/high-*TaMOR*) and *HapC4* (high-*TaMIP1*/high-*TaMOR*), suggesting that the effect of *TaMOR* haplotypes is epistatic to that of *TaMIP1* haplotypes on the RDW (Fig. 7g). We also analyzed spike length of the 4 combinations in various environments and found that *HapC2* (*TaMIP1-Hap*-2A-1/*TaMOR*-MITE^{-}) had the longest spike among them (Fig. 7h). Furthermore, the distribution analysis of the 4 combinations in landraces and modern cultivars showed that the ratio of *HapC2* significantly increased in the 10 major wheat zones except the Xinjiang Winter-Spring Wheat Zone (X) (Fig. 7i). The results revealed that *TaMIP1* and *TaMOR* haplotypes have additive effects on RDW, and the effect of *TaMOR* haplotypes is epistatic to that of *TaMIP1* haplotypes. The *HapC2* with the longest spike and high RDW has been positively selected in the Chinese breeding process.

Discussion

Root system architecture is regarded as a main target of the next green revolution due to the role of roots in water and nutrient absorption (Villordon et al. 2014). Root length density and surface area, determined by root number, are essential traits for the improvement of drought resistance and yield in crops (Comas et al. 2013; Zhu et al. 2018). Gene exploration and functional analysis provide opportunities for root number optimization in various environments which is restrained by difficulties in phenotypic identification. Here, the bHLH transcription factor TaMIP1 was identified as a regulator of root development responsive to drought stress through transcriptome and association analysis (Fig. 1). It is a key factor regulating the number of crown roots and lateral roots, and trade-off between yield and drought resistance.

The plant bHLH transcription factors, with DNA binding domains and activity domains, function as transcription regulators of gene expression in multiple biological processes (Gao et al. 2024). Root plasticity is important for plant adaptation and survival under abiotic stress (Gupta et al. 2020; Karlova et al. 2021). This work demonstrated that expression of TaMIP1 was significantly repressed in the root which growth was hampered under drought stress (Fig. 1 and Fig. 2a). It interacts with TaMOR and promotes crown and lateral root number by regulating expression of genes involved in auxin signaling pathway and root development (Figs. 2, 3, and 5). The genes involved in root development, *LBD13*, *LBD15*, *SHR1*, *SCR1*, *GATA4*, *BRN2*, *PIN2*, and *TaMOR*, are targets of TaMIP1. TaMIP1 directly induces their expression by specifically binding to the E-box CATATG, CAATTG, and CAGTTG in the promoters (Fig. 6). The LBD proteins LBD16 and LBD18 are important regulatory factors for the initiation and development of roots downstream of *AUXIN1* (AUX1) and *LIKE-AUXIN3* (LAX3) (Lee et al. 2015). LBD18 directly induces *EXPANSIN14* (EXP14) expression to promote the appearance of lateral roots in Arabidopsis (Lee et al. 2013). The wheat LBD protein TaMOR interacts with ARF5 to directly induce *PIN2* expression to enhance crown root development (Li et al. 2022). The GATA transcription factor GATA23, specifically expressed in xylem pole pericycle cells, controls the identity of lateral root founder cell specification in the Aux/IAA28-dependent auxin signaling pathway in meristematic tissues (Rybel et al. 2010). SHR and SCR, which are required for formative divisions in the stem cell niche of roots, coordinate root patterning to regulate development of primary, lateral, and adventitious roots in Arabidopsis (Lucas et al. 2011; Winter et al. 2024). Therefore, *TaMIP1* is crucial for the root plasticity regarding crown root and lateral root number under drought stress. The molecular mechanism of *TaMIP1* controlling plasticity of crown root and lateral root number is a basis for optimizing the root system architecture.

Increasing root biomass enhances drought resistance and yield under WL conditions (Lee et al. 2017), but an excessive root system may have negative effects on the aboveground growth and yield (Dolferus 2014). The decrease of root number and root to shoot ratio in the modern wheat breeding for high yield indicates that the trade-off between underground and aboveground exists (Zhu et al. 2018; Fradgley et al. 2020). However, the genetic control and underlying

molecular mechanisms of the trade-offs between root biomass and yield, as well as drought resistance and yield, remain largely uncharacterized. In this study, we found that TaMIP1 modulates the trade-offs of root number, drought resistance, and yield. Besides fewer roots, *mip1* mutants exhibited improved grain yield under WW conditions but decreased drought resistance coefficient of yield per plant under WL conditions (Fig. 4). It promotes crown and lateral root development by regulating the expression of genes involved in auxin signaling pathway and root development (Fig. 5a). Furthermore, the expression levels of the drought-responsive genes *LEA1*, *DHN2*, and *DREB3* and ABA receptor gene *PYL4* were reduced in the *mip1* mutant (Fig. 5b). Promoter sequence analysis showed that there are 1 E-box (5′-CATATG-3′) in *DREB3* and 1 E-boxes (5′-CAATTG-3′) in *PYL4* targeted by TaMIP1 (Fig. S6a and S6b), suggesting they are directly regulated by TaMIP1. Thus, TaMIP1 integrates auxin and ABA signaling to confer the trade-offs of root number, drought resistance and yield. The phenotype analysis of overexpression and backcross wheat lines revealed that *TaDREB3* has positive effects on survival rate and grain yield under WL conditions and no impact on growth and grain yield under WW conditions (Shavrukov et al. 2016). Compared with WT, overexpression of *TaPYL4* increased yield, and knockdown lines exhibited decreased yield under WL conditions. Under WW conditions, the yield of *TaPYL4* transgenic lines was similar to that of WT. Upregulation of root system architecture genes was associated with the *TaPYL4*-enhanced drought adaptation (Zhang et al. 2022). The findings help us to hypothesize that in the *mip1* mutant, employing drought-inducible promoters to induce expression of *DREB3* and *PYL4* is an effective strategy for breeding high-yielding and drought-resistant wheat cultivars. Therefore, the TaMIP1-*DREB3*/*PYL4* regulatory module provides molecular targets to improve drought resistance and yield in wheat.

Identifying natural allelic variations of functional genes and analyzing their impacts on phenotype and molecular mechanisms are the basis and efficient ways in molecular breeding (Mei et al. 2022). In this study, 2 haplotypes of *TaMIP1* were identified in the wheat natural population. There are 2 non-synonymous SNPs in *TaMIP1* coding sequence, which make that TaMIP1$^{Hap\text{-}2A\text{-}2}$ has higher transactivation activity of target genes than TaMIP1$^{Hap\text{-}2A\text{-}1}$, leading to higher root dry weight and shorter spike of *Hap*-2A-2 genotype compared with *Hap*-2A-1 genotype (Fig. 1d-f, Fig. S7a and Fig. 7a-d). In the process of Chinese wheat breeding, *Hap*-2A-1 genotype with longer spike but lower root dry weight has been positively selected in the regions with sufficient water supply, which explains the molecular basis for decreased root number in modern cultivars. The *Hap*-2A-2 genotype with higher root dry weight but shorter spike has been positively selected in the Northern Spring Wheat Zone (VII), Qinghai-Tibetan Plateau Spring-Winter Wheat Zone (IX), and Xinjiang Winter-Spring Wheat Zone (X) in the arid and semi-arid regions (Fig. 7e). Moreover, analysis of the combined haplotypes revealed the additive effects of *TaMIP1* and *TaMOR* haplotypes and the epistatic effect of *TaMOR* haplotypes on RDW. Finally, we found *HapC2* (low-*TaMIP1*/high-*TaMOR*) with the longest spike and high RDW is pivotal in overcoming the trade-off between underground and aboveground growth, as well as drought resistance and yield (Fig. 7f-i).

Taken together, we propose a model to demonstrate the role of *TaMIP1* in the regulation of root density, drought resistance and yield (Fig. 7j). In WT, TaMIP1 directly induces expression of auxin transporter gene *PIN2*, root development genes *TaMOR*, *BRN2*, *GATA4*, *LBDs*, *SCR1*, and *SHR1*; drought-responsive gene *DREB3*; and ABA receptor gene *PYL4* by binding to the specific E-box in their promoters. The induction of *BRN2*, *PIN2*, and *TaMOR* expression was enhanced by TaMOR-TaMIP1. The expression levels of the target genes in *Hap*-2A-2 genotype are higher than that in *Hap*-2A-1 genotype because of the higher transactivation activity of TaMIP1$^{Hap\text{-}2A\text{-}2}$. However, in *mip1* mutants, the expression levels of target genes are very low, leading to decreased root biomass and high yield under WW conditions. Under WL conditions, *mip1* are hypersensitive to drought with lower survival rate and drought resistance coefficient of yield per plant. This work advances our understanding of the molecular regulation of root development and the trade-off between drought resistance and yield and provides genetic resources to breed drought resistant and high-yielding wheat.

Materials and methods

Plant materials and phenotyping

The wheat cultivar Jinmai 47 was selected for PEG treatment. The seedlings of Jinmai 47 were hydroponically cultivated in Hoagland nutrient solution for 3 d and transferred to the 20% PEG solution for 6 d in the artificial climate chamber at 23 °C, 16 h/20 °C, 8 h (light/darkness). The root phenotypes were identified by the scanner (EPSON EXPRESSION 10,000 XL, Japan), and roots were sampled for RNA sequencing.

The wheat cultivar Hanxuan10 was used for gene expression analysis. For the analysis at seedling stage, tissues were collected from seedlings hydroponically cultivated in an artificial climate chamber at 23 °C, 16 h/20 °C, 8 h (light/darkness) for 2 wk. For analysis at jointing, heading and flowering stage, seeds were sowed in polyvinyl chloride (PVC) pipes in Beijing. Tissues were sampled from plants at the jointing, heading and flowering stages, respectively. For expression analysis under treatments, 2-wk-old seedlings were treated by 0.1 mM IAA, 50 μM ABA, and 16.1% PEG-*A*, -*B*, and -*D* (Li et al. 2019a). Population 2 consisting of 323 wheat accessions was used for association analysis (Li et al. 2019b). A total 157 landraces and 348 modern cultivars were used to analyze the distribution of gene haplotypes (Hao et al. 2011).

To generate *TaMIP1* mutants, 4 primers containing two 19-bp gene-specific sequences of *TaMIP1-A*, *-B*, and *-D* were designed to clone the fragment of pCBC-MT1T2 to the CRISPR/Cas9 vector pBUE414 targeting *TaMIP1-A*, *-B*, and *-D*, and then transformed into wheat cultivar Fielder. Three homozygous mutant lines were identified by PCR and sequencing for phenotyping. Seedlings were hydroponically cultured for 10 d to investigate root traits at seedling stage. For phenotypes at booting stage and grain filling stage, seeds were sowed in PVC pipes in field and phenotyped at booting stage and grain filling stage. The root number represents the number of crown roots and seminal roots. For the mature phenotypes, seeds were planted in Shunyi (Beijing) transgenic experimental fields, and phenotypes such as plant height, spike length, tiller number, spikelet number per spike, and grain number per spike were investigated. After harvest, grain yield per plant and 1000-grain weight were investigated. Drought treatment of seedlings was performed in the container (56 cm × 38 cm × 11 cm) in Beijing. Drought treatment started at 3-leaf stage by stopping watering. The seedlings were rewatered after 18 d of drought, and then survival seedlings were investigated on the fourth day.

The coding sequence (CDS) of *TaMIP1* from the wheat cultivar Chinese Spring was cloned into the pCUbi1390 vector and

transformed to the Japonica rice variety Kitaake. Two T3 homozygous lines (OE-12 and OE-20) were obtained by hygromycin screening and PCR detection for phenotypes.

Quantitative real-time PCR assay

Total RNA was extracted by the RNA extraction kit (ZP405 K, ZOMANBIO), and cDNA was synthesized using FastQuant RT kit (KR116, TIANGEN). Specific primers of target genes and internal control *TaTUBULIN* (*TaTUB*) (Table S2) were designed, and real-time qPCR experiments were performed using SYBR Premix Ex Taq reagent according to the instructions with LightCycler 96 System (Roche).

Subcellular localization

The full-length CDS of *TabHLH112-2A* were cloned into the vector pCAMBIA1300, transformed into *Agrobacterium tumefaciens* strain EHA105, and infiltrated into *Nicotiana benthamiana* leaves. EHA105 with pCAMBIA1300-H2B-mCherry was co-infiltrated as a nuclear marker. After 48 h, fluorescence signal was detected using a confocal microscope (LSM880, Carl Zeiss). Primers are listed in Table S2.

Transactivation activity assay

Full-length CDS and truncated fragments encoding 1-307 aa and 308 to 435 aa of TabHLH112-2A were cloned into pGBKT7 to construct BD-TabHLH112-2A, BD-TabHLH112-2A-1, and BD-TabHLH112-2A-2 and co-transformed with pGADT7 into the yeast strain Y2HGold, separately. The yeast co-transformed with pGBKT7 and pGADT7 vector was used as negative control. The transformed yeasts were incubated on SD-Trp/Leu and SD-Trp/Leu/His/Ade medium at 30 °C. Primers are listed in Table S2.

Yeast 2-hybrid assay

For the yeast 2-hybrid screening assay, BD-TabHLH112-2A-2 was used as bait to screen the cDNA prey library obtained from wheat roots and root bases. Positive clones were identified by PCR and sequencing with primers T7 and 3AD.

In the yeast two-hybrid assay, the CDS of *TabHLH112-2A* was cloned into pGADT7 to construct AD-TabHLH112-2A, co-transformed with BD-TaMOR210 into yeast strain Y2HGold. Empty vector pGBKT7 and pGADT7 were used as negative controls. The transformed yeast was cultured on SD-Trp/Leu and SD-Trp/Leu/His/Ade medium for 3 d at 30 °C. Primers are listed in Table S2.

Luciferase complementation imaging assay

The CDS of *TabHLH112-2A* and *TaMOR* were cloned into pCAMBIAI1300-cLUC and pCAMBIAI1300-nLUC vectors to form cLUC-TabHLH112-2A and TaMOR-nLUC. They were transformed into EHA105 and infiltrated into *Nicotiana benthamiana* leaves. Empty pCAMBIAI1300-cLUC and pCAMBIAI1300-nLUC vectors were used as negative controls. After 48 h, transfected leaves were sprayed with the substrate (10 mM luciferin), incubated in darkness for 5 min, and then photographed with imaging apparatus (NightShade LB 985, Berthold). Primers are listed in Table S2.

Bimolecular fluorescence complementation assay

The CDS of *TabHLH112-2A* and *TaMOR* were fused to the C-terminal fragment of YFP (YCE) and N-terminal fragment of YFP (YNE), respectively. They were introduced into EHA105 and co-transformed to *N. benthamiana* leaves. Transfected leaves were detected by the confocal microscope (LSM880, Carl Zeiss) after 48 h. Primers are listed in Table S2.

Co-immunoprecipitation assay (CoIP)

The CDS of *TabHLH112-2A* and *TaMOR* were cloned into vector pCAMBIA1300-Flag and pCAMBIA1300-GFP to form TabHLH112-2A-Flag and TaMOR-GFP, respectively. They were introduced into *Agrobacterium tumefaciens* strain EHA105 and infiltrated into *N. benthamiana* leaves. After 48 h, the infiltrated leaves were ground to powder in liquid nitrogen and resuspended in protein extraction buffer. Anti-GFP (598-7, MBL) and anti-Flag (M185-7, MBL) antibodies were used to detect the expression of TaMOR-GFP and TabHLH112-2A-Flag as input. GFP beads (D153-11, MBL) were added and incubated at 4 °C for 2 h. After incubation, the beads were washed in PBS and detected by western-blot analysis.

Methylene blue staining

To observe the lateral root primordia, methylene blue staining was performed. After culturing the seedlings in Hoagland nutrient solution for 3 d, samples were taken from the roots at a distance of 2 to 4 cm from the root tip. The samples were fixed in FAA at 4 °C for 24 h. After fixation, the seedlings were washed 3 times with ddH_2O for 10 min each time, then transferred to 0.01% methylene blue solution for 5 min, washed with ddH_2O for 10 min, and finally imaged using a stereo microscope (SteREO Discovery.V20, Zeiss).

Transcriptomic analysis

Total RNA was isolated using RNA Extraction Kit (ZP405 K, ZOMANBIO). The RNA quantification, qualification, library preparation and 150-bp paired-end sequencing was performed at Azenta (Beijing). Differential expression of genes was analyzed with the DESeq2 Bioconductor package. GOSeq (v1.34.1) was used to identify GO (Gene Ontology) terms that annotate a list of enriched genes with a significant padj less or equal than 0.05.

Yeast 1-hybrid assay

The CDS of *TaMIP1* were cloned into the pB42AD vector. The promoter sequences of *LBD13*, *SHR1*, *CRL5*, *LBD15*, *GATA2*, *BRN2*, *AT23*, *GATA4*, and *SCR1* were inserted into the pLacZi vector. They were co-transformed into the yeast strain EGY48. The yeast strains were incubated on SD-Trp/Ura medium for 3 d and transferred on SD-Trp/Ura medium containing 20 mM X-gal (5-bromo-4-chloro-3-indolyl-β-D-galactopyranoside).

Dual luciferase reporter assay

TaMIP1-GFP and TaMOR-GFP were used as effectors. The promoter sequences of *BRN2*, *LBD13*, *SCR1*, *SHR1*, *MOR*, and *GATA4* were clone into pGreenII 0800-LUC vector to construct the reporter. pCAMBIA1300-GFP was used as vector control. They were introduced into *Agrobacterium tumefaciens* strain GV3101 and infiltrated into *N.benthamiana* leaves. The signals of LUC and REN were detected with Dual-Glo Luciferase Assay System (E2920, Promega). The ratio of LUC to REN was analyzed as relative luciferase activity.

Electrophoretic mobility shift assay (EMSA)

The coding sequence of *TaMIP1* was cloned into vector pGEX4T-1 to construct GST-TaMIP1. GST-TaMIP1 and the empty GST vector pGEX4T-1 were separately transformed into the *E. coli* strain Rosetta. The GST-TaMIP1 and GST proteins were induced by 0.5 mM IPTG at 28 °C. The probes were synthesized by BGI. The assay was performed using the LightShift Chemiluminescent EMSA Kit (20148, Thermo). Primers and probes are listed in Table S2.

Molecular marker development and association analysis

The specific primers of *TabHLH112-2A*, *2B*, and *2D* genomic sequences were designed to detect the nucleotide polymorphisms in the Population 1 (Table S2). Based on the detected SNP, specific molecular marker primers TabHLH112-2A-PvuII-F/R were developed using dCAPS Finder 2.0 (http://helix.wustl.edu/dcaps/dcaps.html) (Table S2). The genome sequences of Population 1 were amplified with TabHLH112-2A-F/R. The PCR products were used as the templates for the second round PCR with TabHLH112-2A-PvuII-F/R primers. The second-round PCR products were digested with *Pvu*II to distinguish haplotypes according to the size of the digested products.

Genotypes of Population 2 were detected by the developed molecular marker. Association analysis was performed by general linear model (GLM) in software TASSEL 5 with $P < 0.05$ as significant association threshold. The significance of phenotypic differences between 2 genotypes was calculated by Student *t* test.

Accession numbers

Sequence data from this article can be found in the GenBank/EMBL data libraries under accession numbers listed in Table S3.

Acknowledgments

Thanks to Professor Chenyang Hao and Tian Li (Institute of Crop Sciences, Chinese Academy of Agricultural Sciences) for providing the wheat population and for the revision suggestions.

Author contributions

C. L. and R. J. supervised the project. Z. F. and C.L. designed the research and wrote the paper. Z. F. and X. T. performed experiments. J. W., Y. Z., W. A., Y. J., Z. P., Y. W., L. L., X. M., D. S., J. X. and M. P. R. helped with the preparation of plant materials, data analysis and manuscript revision. All authors discussed the results and commented on the manuscript.

Supplementary material

Supplementary material is available at *Plant Physiology* online.

Funding

This work was supported by the Biological Breeding-National Science and Technology Major Project (2023ZD0407101), the National Natural Science Foundation of China (32472057 and 32061143040), the National Key R&D Program of China (2021YFD1200603), and the Youth Innovation Program of Chinese Academy of Agricultural Sciences (Y2023QC01).

Conflicts of interest

The authors declare no conflicts of interest.

Data availability

The data supporting the findings of this study are available from the corresponding author upon request.

References

Akpinar BA, Lucas S, Hikmet B. 2013. Genomics approaches for crop improvement against abiotic stress. *Sci World J*. 2013:361921.

Budak H, Hussain B, Khan Z, Ozturk NZ, Ullah N. 2015. From genetics to functional genomics: improvement in drought signaling and tolerance in wheat. *Front Plant Sci*. 6:1012. https://doi.org/10.3389/fpls.2015.01012.

Castilhos G, Lazzarotto F, Spagnolo-Fonini L, Bodanese-Zanettini M, Margis-Pinheiro M. 2015. Possible roles of basic helix-loop-helix transcription factors in adaptation to drought. *Plant Sci*. 235:130–130. https://doi.org/10.1016/j.plantsci.2015.03.012.

Comas L, Becker S, Cruz V, Byrne P, Dierig D. 2013. Root traits contributing to plant productivity under drought. *Front Plant Sci*. 4:442. https://doi.org/10.3389/fpls.2013.00442.

Dolferus R. 2014. To grow or not to grow: a stressful decision for plants. *Plant Sci*. 229:247–261. https://doi.org/10.1016/j.plantsci.2014.10.002.

Du H *et al.* 2012. A GH3 family member, OsGH3-2, modulates auxin and abscisic acid levels and differentially affects drought and cold tolerance in rice. *J Exp Bot*. 63:6467–6480. https://doi.org/10.1093/jxb/ers300.

Du L *et al.* 2023. TaERF87 and TaAKS1 synergistically regulate TaP5CS1/TaP5CR1-mediated proline biosynthesis to enhance drought tolerance in wheat. *New Phytol*. 237:232–250. https://doi.org/10.1111/nph.18549.

Fan ZP *et al.* 2024. Cloning of *TabHLH112-2B* gene and development of its functional marker associated with the number of spikelet per spike in wheat. *Acta Agron Sin*. 50:403–413. https://doi.org/10.3724/SP.J.1006.2024.31016.

Fradgley N *et al.* 2020. Effects of breeding history and crop management on the root architecture of wheat. *Plant Soil*. 452:587–600. https://doi.org/10.1007/s11104-020-04585-2.

Gao F, Dubos C. 2024. The arabidopsis bHLH transcription factor family. *Trends Plant Sci*. 29:668–680. https://doi.org/10.1016/j.tplants.2023.11.022.

Gao J *et al.* 2023. RRS1 shapes robust root system to enhance drought resistance in rice. *New phytol*. 238:1146–1162. https://doi.org/10.1111/nph.18775.

Guo XJ, Wang JR. 2017. Global identification, structural analysis and expression characterization of bHLH transcription factors in wheat. *BMC Plant Biol*. 17:90. https://doi.org/10.1186/s12870-017-1038-y.

Gupta A, Rico-Medina A, Caño-Delgado AI. 2020. The physiology of plant responses to drought. *Science*. 368:266–269. https://doi.org/10.1126/science.aaz7614.

Hao CY, Wang LF, Ge HM, Dong YC, Zhang XY. 2011. Genetic diversity and linkage disequilibrium in Chinese bread wheat (*Triticum aestivum* L.) revealed by SSR markers. *PLoS One*. 6:e17279. https://doi.org/10.1371/journal.pone.0017279.

Herder GD, Isterdael GV, Beeckman T, Smet ID. 2010. The roots of a new green revolution. *Trends Plant Sci*. 15:600–607. https://doi.org/10.1016/j.tplants.2010.08.009.

Inukai Y *et al.* 2005. *Crown rootless1*, which is essential for crown root formation in rice, is a target of an AUXIN RESPONSE FACTOR in auxin signaling. *Plant Cell*. 17:1387–1396. https://doi.org/10.1105/tpc.105.030981.

Karlova R, Boer D, Hayes S, Testerink C. 2021. Root plasticity under abiotic stress. *Plant Physiol*. 187:1057–1070. https://doi.org/10.1093/plphys/kiab392.

Kitomi Y *et al.* 2011. The auxin responsive AP2/ERF transcription factor CROWN ROOTLESS5 is involved in crown root initiation in rice through

the induction of *OsRR1*, a type-A response regulator of cytokinin signaling. *Plant J*. 67:472–484. https://doi.org/10.1111/j.1365-313X.2011.04610.x.
Kumar R, Mukherjee S, Ayele BT. 2018. Molecular aspects of sucrose transport and its metabolism to starch during seed development in wheat: a comprehensive review. *Biotechnol Adv*. 36:954–967. https://doi.org/10.1016/j.biotechadv.2018.02.015.
Lee DK *et al.* 2017. The rice OsNAC6 transcription factor orchestrates multiple molecular mechanisms involving root structural adaptions and nicotianamine biosynthesis for drought tolerance. *Plant Biotechnol J*. 15:754–764. https://doi.org/10.1111/pbi.12673.
Lee HW, Cho C, Kim J. 2015. *Lateral organ boundaries domain16* and *18* act downstream of the AUXIN1 and LIKE-AUXIN3 auxin influx carriers to control lateral root development in Arabidopsis. *Plant Physiol*. 168:1792–1806. https://doi.org/10.1104/pp.15.00578.
Lee HW, Kim MJ, Kim NY, Lee SH, Kim J. 2013. LBD18 acts as a transcriptional activator that directly binds to the *EXPANSIN14* promoter in promoting lateral root emergence of Arabidopsis. *Plant J*. 73:212–224. https://doi.org/10.1111/tpj.12013.
Li CN *et al.* 2021. Recognizing the hidden half in wheat: root system attributes associated with drought tolerance. *J Exp Bot*. 72:5117–5133. https://doi.org/10.1093/jxb/erab124.
Li CN *et al.* 2022. TaMOR is essential for root initiation and improvement of root system architecture in wheat. *Plant Biotechnol J*. 20:862–875. https://doi.org/10.1111/pbi.13765.
Li L *et al.* 2019a. Genetic dissection of drought and heat-responsive agronomic traits in wheat. *Plant Cell Environ*. 42:2540–2553. https://doi.org/10.1111/pce.13577.
Li L *et al.* 2019b. Genome-wide association study reveals genomic regions controlling root and shoot traits at late growth stages in wheat. *Ann Bot*. 124:993–1006. https://doi.org/10.1093/aob/mcz041.
Liu H, Yang Y, Liu DD, Wang XY, Zhang LS. 2020. Transcription factor TabHLH49 positively regulates dehydrin *WZY2* gene expression and enhances drought stress tolerance in wheat. *BMC Plant Biol*. 20:259. https://doi.org/10.1186/s12870-020-02474-5.
Lucas M *et al.* 2011. Short-root regulates primary, lateral, and adventitious root development in Arabidopsis. *Plant Physiol*. 155:384–398. https://doi.org/10.1104/pp.110.165126.
Lynch J. 2013. Steep, cheap and deep: an ideotype to optimize water and N acquisition by maize root systems. *Ann Bot*. 112:347–357. https://doi.org/10.1093/aob/mcs293.
Ma H *et al.* 2018. ZmbZIP4 contributes to stress resistance in maize by regulating ABA synthesis and root development. *Plant physiol*. 178:753–770. https://doi.org/10.1104/pp.18.00436.
Mao H *et al.* 2022. The wheat ABA receptor gene *TaPYL1-1B* contributes to drought tolerance and grain yield by increasing water-use efficiency. *Plant Biotechnol J*. 20:846–861. https://doi.org/10.1111/pbi.13764.
Mao H *et al.* 2020. Regulatory changes in TaSNAC8-6A are associated with drought tolerance in wheat seedlings. *Plant Biotechnol J*. 18:1078–1092. https://doi.org/10.1111/pbi.13277.
Mei F *et al.* 2022. A gain-of-function allele of a DREB transcription factor gene ameliorates drought tolerance in wheat. *Plant Cell*. 34:4472–4494. https://doi.org/10.1093/plcell/koac248.
Norén L *et al.* 2016. Circadian and plastid signaling pathways are integrated to ensure correct expression of the CBF and COR genes during photoperiodic growth. *Plant Physiol*. 171:1392–1406. https://doi.org/10.1104/pp.16.00374.
Olvera-Carrillo Y, Reyes J, Covarrubias A. 2011. Late embryogenesis abundant proteins: versatile players in the plant adaptation to water limiting environments. *Plant Signal Behav*. 6:586–589. https://doi.org/10.4161/psb.6.4.15042.
Placido D, Sandhu J, Sato S, Nersesian N, Walia H. 2020. The *LATERAL ROOT DENSITY* gene regulates root growth during water stress in wheat. *Plant Biotechnol J*. 18:1955–1968. https://doi.org/10.1111/pbi.13355.
Riyazuddin R, Nisha N, Singh K, Verma R, Gupta R. 2022. Involvement of dehydrin proteins in mitigating the negative effects of drought stress in plants. *Plant Cell Rep*. 41:519–533. https://doi.org/10.1007/s00299-021-02720-6.
Rybel BD *et al.* 2010. A novel aux/IAA28 signaling cascade activates GATA23-dependent specification of lateral root founder cell identity. *Curr Biol*. 20:1697–1706. https://doi.org/10.1016/j.cub.2010.09.007.
Shao A *et al.* 2017. The auxin biosynthetic *TRYPTOPHAN AMINOTRANSFERASE RELATED TaTAR2.1-3A* increases grain yield of wheat. *Plant Physiol*. 174:2274–2288. https://doi.org/10.1104/pp.17.00094.
Shao Y *et al.* 2019. OsSPL3, an SBP-domain protein, regulates crown root development in rice. *Plant Cell*. 31:1257–1275. https://doi.org/10.1105/tpc.19.00038.
Shavrukov Y, Baho M, Lopato S, Langridge P. 2016. The TaDREB3 transgene transferred by conventional crossings to different genetic backgrounds of bread wheat improves drought tolerance. *Plant Biotechnol J*. 14:313–322. https://doi.org/10.1111/pbi.12385.
Shewry P, Hey S. 2015. The contribution of wheat to human diet and health. *Food Energy Secur*. 4:178–202. https://doi.org/10.1002/fes3.64.
Thorup-Kristensen K *et al.* 2020. Digging deeper for agricultural resources, the value of deep rooting. *Trends Plant Sci*. 25:406–417. https://doi.org/10.1016/j.tplants.2019.12.007.
Usman B *et al.* 2020. Precise editing of the *OsPYL9* gene by RNA-guided Cas9 nuclease confers enhanced drought tolerance and grain yield in rice (*Oryza sativa* L.) by regulating circadian rhythm and abiotic stress responsive proteins. *Int J Mol Sci*. 21:7854. https://doi.org/10.3390/ijms21217854.
Villordon A, Ginzberg I, Firon N. 2014. Root architecture and root and tuber crop productivity. *Trends Plant Sci*. 19:419–425. https://doi.org/10.1016/j.tplants.2014.02.002.
Wang D *et al.* 2024. TabHLH27 orchestrates root growth and drought tolerance to enhance water use efficiency in wheat. *J Integr Plant Biol*. 66:1295–1312. https://doi.org/10.1111/jipb.13670.
Wang JP *et al.* 2023. The wheat basic helix-loop-helix gene *TabHLH123* positively modulates the formation of crown roots and is associated with plant height and 1000-grain weight under various conditions. *J Exp Bot*. 74:2542–2555. https://doi.org/10.1093/jxb/erad051.
Wang XS *et al.* 2007. Genome-scale identification and analysis of *LEA* genes in rice (*Oryza sativa* L.). *Plant Sci*. 172:414–420. https://doi.org/10.1016/j.plantsci.2006.10.004.
Wasson AP *et al.* 2012. Traits and selection strategies to improve root systems and water uptake in water-limited wheat crops. *J Exp Bot*. 63:3485–3498. https://doi.org/10.1093/jxb/ers111.
Wei K, Chen H. 2018. Comparative functional genomics analysis of bHLH gene family in rice, maize and wheat. *BMC Plant Biol*. 18:309. https://doi.org/10.1186/s12870-018-1529-5.
Winter CM *et al.* 2024. SHR and SCR coordinate root patterning and growth early in the cell cycle. *Nature*. 626:611–616. https://doi.org/10.1038/s41586-023-06971-z.
Ye H *et al.* 2018. Genetic diversity of root system architecture in response to drought stress in grain legumes. *J Exp Bot*. 69:3267–3277. https://doi.org/10.1093/jxb/ery082.
Zhang Y *et al.* 2022. *TaPYL4*, an ABA receptor gene of wheat, positively regulates plant drought adaptation through modulating the osmotic stress-associated processes. *BMC Plant Biol*. 22:423. https://doi.org/10.1186/s12870-022-03799-z.
Zhu YH, Weiner J, Yu MX, Li FM. 2018. Evolutionary agroecology: trends in root architecture during wheat breeding. *Evol Appl*. 12:733–743. https://doi.org/10.1111/eva.12749.